Structural and physical properties of the metal (M) substituted $YBa_2Cu_{3-x}M_xO_{7-y}$ perovskite

J. M. Tarascon, P. Barboux, P. F. Miceli, L. H. Greene, and G. W. Hull
Bell Communications Research Inc., 331 Newman Springs Road, Red Bank, New Jersey 07701

M. Eibschutz and S. A. Sunshine
AT&T Bell Laboratories, Murray Hill, New Jersey 07974
(Received 24 December 1987)

The mixed $YBa_2Cu_{3-x}M_xO_{7-y}$ (M=Ni, Zn, Fe, Co, and Al) phases have been characterized for their structural, magnetic, and superconducting properties. The oxygen content in these phases is dependent on the nature and the amount of doping, especially for Co and Fe. The material remains orthorhombic when Cu is replaced by Ni or Zn whereas it evolves to tetragonal symmetry for the Fe-, Co- and Al-doped compounds when x exceeds 0.05. Evidence for the major substitution of Co in the Cu—O chains only is obtained by means of thermogravimetric analysis and neutron diffraction measurements. The room-temperature Mössbauer spectra of the Fe-doped compounds consist of three doublets; their site assignments are proposed. dc resistance and ac susceptibility have shown that both magnetic and diamagnetic ions destroy T_c in a similar manner. At x=0.2 the Fe and Co compounds are tetragonal, superconduct at 50 K, and show a Curie-type magnetic behavior associated with a magnetic moment of $3.4\mu_B$ per doping atom. The origin of the orthorhombic-tetragonal transition and the importance of the Cu—O chains for superconductivity is discussed. The behavior of these materials with respect to magnetic impurities is apparently different from conventional Bardeen-Cooper-Schrieffer-type superconductors, and we believe that any new mechanism proposed must be mostly sensitive to local structural disorder.

INTRODUCTION

The oxygen-defect superconducting perovskites of general formula $MBa_2Cu_3O_{7-y}$ (where M=Y and the rare earths) have revived the field of superconductivity because they exhibit the highest superconducting transition temperatures (T_c=95 K) and the highest onset superconducting critical fields (340 T, extrapolated to 0 K) ever observed.[1,2]

The structure of this material (referred to here as the 90-K material for simplicity) has been determined by means of single-crystal x-ray diffraction[3] and powder neutron diffraction studies.[4-9] It is well established that this phase crystallizes in an orthorhombic unit cell which can be viewed as a packing along the c axis of Y, CuO_2, BaO, CuO, BaO, CuO_2, and Y layers. The oxygen vacancies are ordered within the Cu—O median plane resulting in the existence of Cu—O chains running along the b axis. In the following, for reason of clarity, the copper and oxygen sites belonging to the Cu—O plane sandwiched between the Ba planes will be denoted as Cu(1) and O(1), respectively, and Cu(2) and O(2) for the outer planes. It has been shown[10-13] that these compounds can easily and reversibly accommodate oxygen atoms over the range of composition $0<y<1$. For $7-y\geq 6.8$ the compound is an orthorhombic superconductor. As oxygen is removed, the orthorhombicity is reduced until a tetragonal structure results. The value of y at which this orthorhombic-tetragonal (denoted O-T in the following) structural transition occurs is dependent upon how the oxygen is removed.[14,15] However, the tetragonal structure $MBa_2Cu_3O_{7-y}$ is a semiconductor with oxygen in the central plane partially occupying sites both in the a and b axis (i.e., without chains[11]).

For conventional superconductors[16] the presence of magnetic impurities (which act as pair breakers) destroys T_c, but the chemical substitution of yttrium by rare earths possessing large magnetic moments in $YBa_2Cu_{3-x}M_xO_{7-y}$ has shown no effect on T_c, most likely due to the weak interactions (i.e., large distance) between the rare-earth ions and the superconducting electrons.[10] As band-structure calculations by Matthiess and Hamman[17] have shown, the metallic properties of these materials are mainly governed by the Cu $3d$-O $2p$ electrons, a simple way to shorten this distance is to directly place these magnetic ions on the copper sites. But we have performed such a study for the 40 K ($La_{2-x}Sr_xCuO_{4-y}$) material and found that T_c was depressed even faster for the nonmagnetic ion Zn than for the magnetic ion Ni, leading to the conclusion that these materials have a behavior apparently different than conventional superconductors,[18] and that their superconducting properties are much more sensitive to local structural disorder than to magnetic interactions.

In this paper we report a complete and detailed investigation of the influence of doping on the structural and physical properties of $YBa_2Cu_{3-x}M_xO_{7-y}$ (where M is Fe, Zn, Ni, Co, and Al). Aluminum is used here for comparison to the transition metals because it is a well-defined trivalent ion. We find both a depression of T_c for all dopants and that the Fe-, Co-, and Al-doped phases become tetragonal with increasing x. Some of these results were also observed by Maeno *et al.*[19] We show that for both Fe- and Co-doped materials, the oxygen content (y) changes as a function of doping content x, whereas no major changes are detected in the case of Zn or Ni.

Thermogravimetric analysis, powder x-ray diffraction, powder neutron diffraction magnetic susceptibility, and

Mössbauer measurements were used to determine the position of the doping ions within the unit cell as well as their oxidation state.

EXPERIMENT

The mixed compounds $YBa_2Cu_{3-x}M_xO_{7-y}$ were prepared by thoroughly mixing appropriate amounts of $BaCO_3$ and corresponding oxide powders, each 99.99% pure. The mixed powders, placed in alumina crucibles, were heated to 960 °C, maintained at this temperature for 48 h, slowly cooled down to 300 °C, and then removed from the furnance. Grinding and firing were repeated until the complete homogeneity of the resulting materials, as determined by powder x-ray diffraction, was ensured. All the Fe, Co, Ni, and Zn substituted samples reported here, except for the compositions $x = 0.02$ and 0.05, received exactly the same heat treatment since they were always handled together.

The resulting powders were characterized by x-ray diffraction in the Bragg-Brentano geometry with Cu $K\alpha$ radiation. The oxygen content in the as-prepared sample was determined both by thermogravimetric analysis (TGA) as described elsewhere[10] and also by the iodometric method.[20] This method (dissolution of the material in an acidified solution of KI followed by back titration of the iodine formed) gives the average oxidation state of the Cu plus the $3d$ metal. From this and the assumption that oxygen has a valence of -2, the total oxygen content is determined. The susceptibility measurements from 4.2 K to room temperature were collected with a superconducting quantum interference device (SQUID) magnetometer. Resistivities were obtained by the standard 4-probe method in an exchange gas cryostat. Superconducting transitions were determined both resistively and magnetically, the latter with an ac-susceptibility bridge operating at a frequency of 13 Hz. The Mössbauer spectra were obtained in transition geometry using a standard constant acceleration spectrometer. The source was ^{57}Co in rhodium metal. The absorbers were powder crystalline materials. Neutron powder diffraction data were collected at room temperature on the Special Environment

TABLE I. Crystallographic lattice parameters and oxygen content, determined both by TGA and chemical analysis for the $YBa_2Cu_{3-x}M_xO_{7-y}$ series studied (M = Fe, Co, Al, Ni, and Zn).

M	x	a (Å)	b (Å)	c (Å)	V (Å^3)	Titration $(7-\delta)$	TGA $(7-\delta)$	$T_c(\rho)$ (K)
Nondoped		3.8146	3.8819	11.6700	172.80	6.85	6.90	92
Fe	0.02	3.8193	3.8836	11.667	173.06	6.93		91.8
	0.05	3.8305	3.8781	11.666	173.31	6.92		91.8
	0.1	3.8598	3.8598	11.863	174.05	6.92		76
	0.2	3.8637	3.8637	11.684	174.41	6.93		49
	0.3	3.8671	3.8671	11.681	174.68	6.96		...
	0.4	3.8707	3.8707	11.674	174.90	7.00		31
	0.5	3.8739	3.8739	11.667	175.09	7.20		0
	0.8	3.8727	3.8727	11.647	174.68	7.25		0
Co	0.02	3.8195	3.8826	11.667	173.02	6.90		93.4
	0.05	3.8295	3.8802	11.670	173.40	6.92		94.3
	0.1	3.8608	3.8608	11.687	174.20	6.82	7.05	73
	0.2	3.8675	3.8675	11.684	174.76	6.83	7.12	53
	0.3	3.8724	3.8724	11.680	174.15	6.88	7.09	22
	0.4	3.8765	3.8765	11.674	175.43	6.95	...	0
	0.5	3.8807	3.8807	11.671	175.75	6.99	7.08	0
	0.8	3.8865	3.8865	11.661	176.13	7.07	7.34	0
	1.0	3.8867	3.8867	11.625	175.61	7.20	...	0
Al	0.05	3.8351	3.8827	11.6822	173.95	6.93		91
	0.1	3.8601	3.8661	11.6750	174.23	6.93		92
	0.2	3.8617	3.8617	11.6727	174.06	6.91		85
	0.3	3.8631	3.8631	11.6719	174.18	6.99		73
	0.4	3.8630	3.8630	11.6713	174.16	7.00		42
Ni	0.1	3.8289	3.8864	11.6372	173.17	6.87		55
	0.2	3.8352	3.8560	11.6573	172.39	6.82		45
	0.3	3.8331	3.8490	11.6624	172.06	6.97		40
Zn	0.1	3.8193	3.8881	11.6818	173.47	6.81		55
	0.2	3.8199	3.8895	11.6804	173.54	6.79		45
	0.3	3.8201	3.8930	11.6797	173.69	6.74		45

Powder Diffractometer (SEPD) at the Intense Pulsed Neutron Source (INPS) of Argonne National Laboratory.

RESULTS

A. X-ray powder diffraction

The crystal data for all the samples reported on this paper are summarized in Table I. For the Ni-, Zn-, and Al-doped compounds the range of solid solution is very small ($0 \leq x \leq 0.3$). The range of solubility is much larger for both Fe ($0 \leq x \leq 0.8$) and Co ($0 \leq x \leq 1$). Extra weak Bragg peaks are detected for the Fe samples with $x \geq 0.8$. Figure 1 shows the variation of the lattice parameters *a*, *b*, and *c* for the Fe, Co, Ni, Zn, and Al series. A striking difference is that the Ni and Zn samples remain orthorhombic throughout their range of existence whereas the Fe, Co, and Al samples undergo a orthorhombic-tetragonal structural phase transition (i.e., *a* becomes equal to *b*) with increasing doping content. The similarity in the structural transition in Fe-, Co-, and Al-doped samples (O-T transition) suggests that Fe and Co, like Al, are trivalent ions. This O-T structural transition occurs over a narrow range of composition as indicated by the sharp anomaly in the *c* lattice parameter, which abruptly increases when *x* reaches 0.05 for Fe and Co, and 0.1 for Al-doped samples. Beyond these values *c* decreases continuously with increasing doping content. In contrast, the *a* lattice parameter within the tetragonal range increases monotonically with increasing either Co or Fe concentration at low *x*, and exhibits a broad maximum near $x = 0.6$ and a level off at $x = 1.0$ for the Fe- and Co-doped phases, respectively. From these data it is tempting to claim that $x = 0.6$ and $x = 1.0$ are the upper limits of solubility for the Fe and Co system, but there are two copper sites in the structure and the preferential filling of one site at low *x* could explain such an effect. Similarly, changes in the electronic configuration (low spin–high spin) of the doping metal with increasing concentration may also lead to similar effects since ion sizes in the high-spin configuration are always greater than those in the low-spin configuration.[20]

The unit-cell volume *V* as a function of doping concentration is shown for each dopant in Fig. 2. *V* decreases with Ni doping and increases with Zn doping as expected from simple ionic radius considerations (as Ni is smaller than Cu which is smaller than Zn). The important result is for the Fe-, Co-, and Al-doped series: although Fe^{3+}, Co^{3+}, and Al^{3+} are each smaller than Cu^{2+} or Cu^{3+}, the volume surprisingly increases with increasing doping concentration. The average valence of copper in the undoped material, determined by charge counting, is 2.33 (assuming an oxygen content of 7 per formula unit and that oxygen has a -2 charge). During the replacement of copper by trivalent ions (Al^{3+}), the copper ions need to be reduced in order to maintain the average charge balance. But another alternative for the charge compensation is an increase of the oxygen content. Both the reduction of the copper valence and an increase in oxygen content will increase the unit-cell volume, as observed.

Finally, Fig. 3 shows what happens to the *a* and *c* lattice

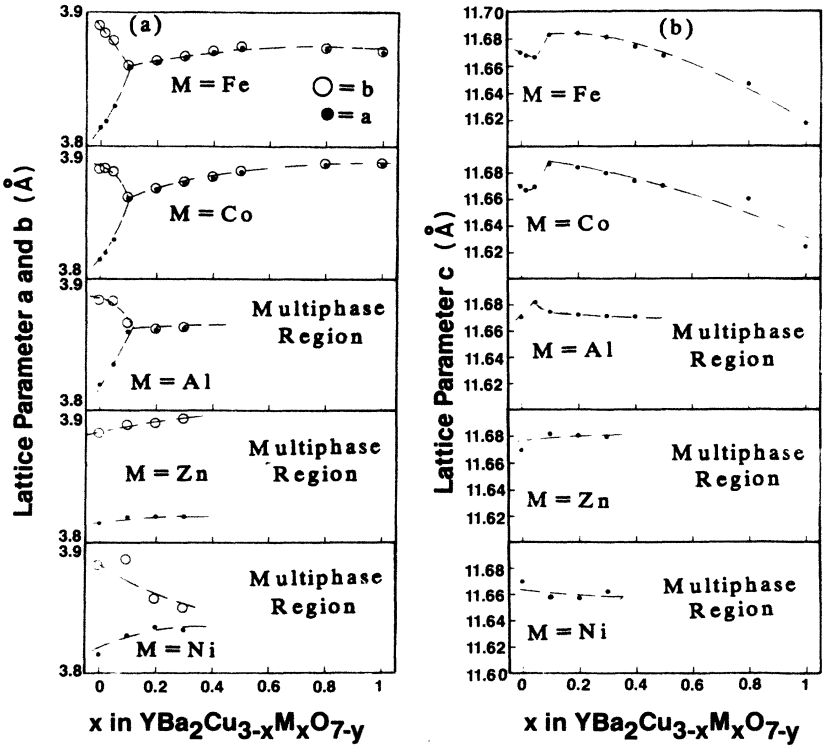

FIG. 1. The unit-cell parameters *a*, *b* and *c* are reported in (a) and (b), respectively, as a function of *x* for the $YBa_2Cu_{3-x}M_xO_{7-y}$ series with M = Fe, Co, Al, Zn, and Ni.

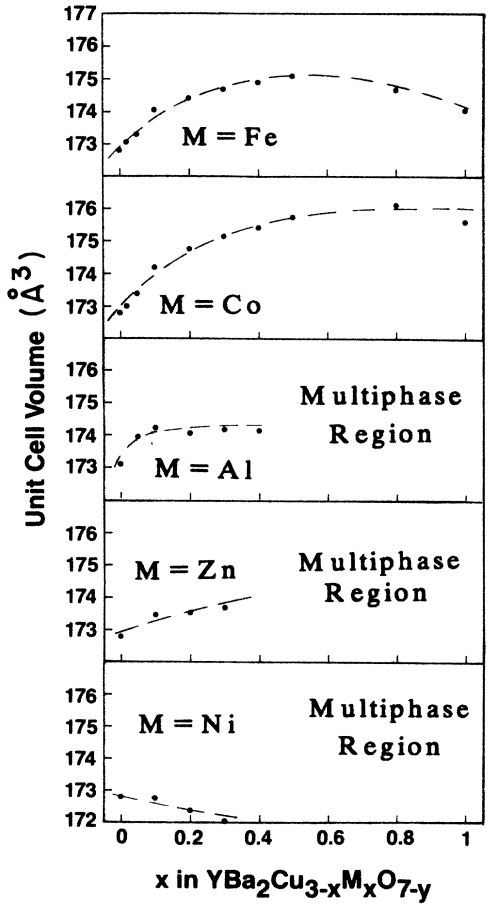

FIG. 2. The unit-cell volume is reported as a function of x for the $YBa_2Cu_3O_{7-y}$ series with M = Fe, Co, Al, Zn, and Ni.

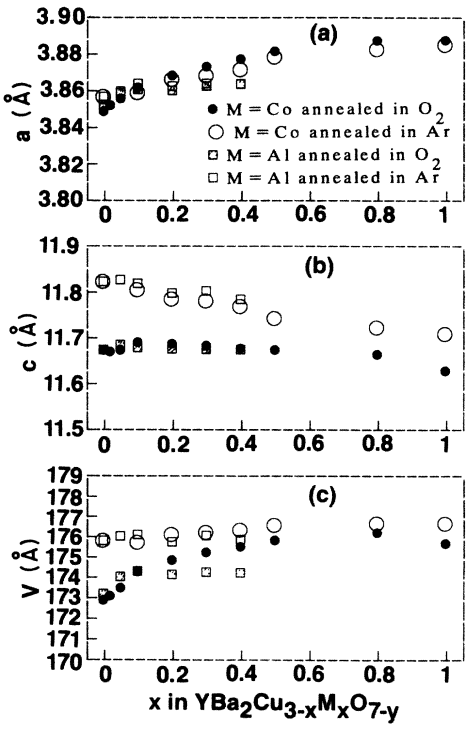

FIG. 3. Tetragonal unit-cell parameters (a, c, V) as a function of x in the $YBa_2Cu_{3-x}M_xO_{7-y}$ series for the as-prepared Co and Al samples (open circles and squares, respectively), and for the same set of samples annealed under argon at 850 °C (solid circles and squares, respectively).

parameters for the Co- and Al-doped samples heated under argon up to 850 °C at a rate of 10 °C/min (i.e., upon removal of oxygen). All the orthorhombic and tetragonal samples become or remain tetragonal. The a lattice parameter remains constant whereas c and V increase considerably. A similar trend was already observed upon removal of oxygen from the undoped material. The removal of oxygen reduces the average valence of copper. Thus, from the smaller valence of Cu one would expect the unit-cell volume to increase, as we observe. It is interesting to note that the volume increase induced by 1 Co per formula unit is identical to that generated by the removal of one oxygen from the undoped material (3 Å^3). Both resulting materials are tetragonal.

B. Thermogravimetric measurements

The oxygen content for the doped samples was determined thermogravimetrically and iodometrically. The results are reported in Table I with the TGA traces shown in Fig. 4. The values of y determined by chemical analysis, which assumed a valence of -2 for oxygen, were systematically low compared to those determined by TGA. As the titration and the TGA always agree in the case of undoped samples, we believe that the discrepancy results from the presence of the dopant (we assumed in the titration that I^- reduces Co^{3+} to Co^{2+}, Fe^{3+} to Fe^{2+}, and does not affect Ni^{2+}, Zn^{2+}, and Al^{3+}). Small amounts of vacancies on the copper sites would also result in low values of y determined chemically. The disagreement in the absolute oxygen values does not affect the following trends: with increasing substitution, within the accuracy

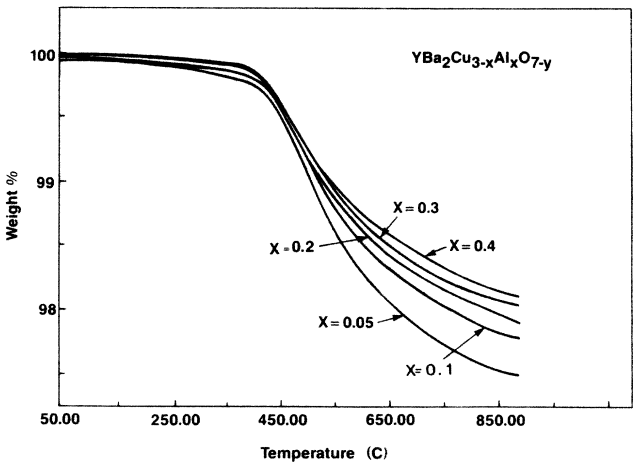

FIG. 4. The TGA traces are shown as function of x for the $YBa_2Cu_{3-x}Al_xO_{7-y}$ series when the sample are heated under argon up to 850 °C at a rate of 10 °C/min.

of the experiments, the oxygen content appears constant at low x, and then increases with increasing Co, Fe, and Al concentration for x greater than 0.2. For increasing concentration of Ni and Zn the oxygen content remains roughly constant and slightly decreases respectively, over their range of existence, $0 \leq x \leq 0.3$ The value of x at which the oxygen content starts to increase does not seem to correlate with the onset of the O-T structural transition.

One oxygen atom per formula unit can be removed within the undoped phase by heating in a low partial presure of oxygen (i.e., argon, vacuum).[10] Since this oxygen is removed only from the Cu—O chains[10] it is expected to be independent of substitutions within the Cu(2)—O planes, but strongly affected by the replacement of copper by other metals within the Cu(1)—O chains due to changes in the strength of the M—O bonds. Thus TGA measurements should be a powerful tool to determine whether the substitution is taking place on Cu(1) or Cu(2) sites. The aluminum system can be used as a test. Single-crystal x-ray studies have been done for the Al-doped samples leading to the result that the Al substitution is taking place on Cu(1) sites.[21] We performed TGA measurements on Al-doped samples by heating the samples under argon up to 850 °C at a rate of 10 °C/min (Fig. 4). We observed that the amount of oxygen removed from the compound decreases monotonically with increasing Al concentration. This is a straightforward indication that the Al ions are going on the chains in agreement with x-ray data. Figure 5 shows similar type of measurements for the Ni-, Zn-, Fe-, and Co-doped samples. The amount of removable oxygen is independent of Ni or Zn concentration. However, a striking result is that it decreases with increasing Fe or Co concentrations, more strongly for the latter. The ever increasing difficulty in removing the oxygen from the Co-doped samples strongly suggests that Co occupies the Cu(1) sites in these chains. For the Fe-doped samples the less dramatic change in oxygen removal with increasing concentration suggests that the substitution most likely occurs on both copper sites. The small changes in the amount of oxygen removed between the $x=0.5$ and $x=0.8$ compounds might indicate that at high x, the substitution is preferentially taking place on the Cu(2) sites. The independence of the oxygen removal to the Ni or Zn concentration does not necessarily suggest that Zn and Ni substitute for Cu in the Cu(2) sites, as will be discussed below. We also find that the removal or uptake of oxygen in the Co-doped samples was perfectly reversible, at least up to heating or cooling rate of 10 °C/min, independent of the doping content.

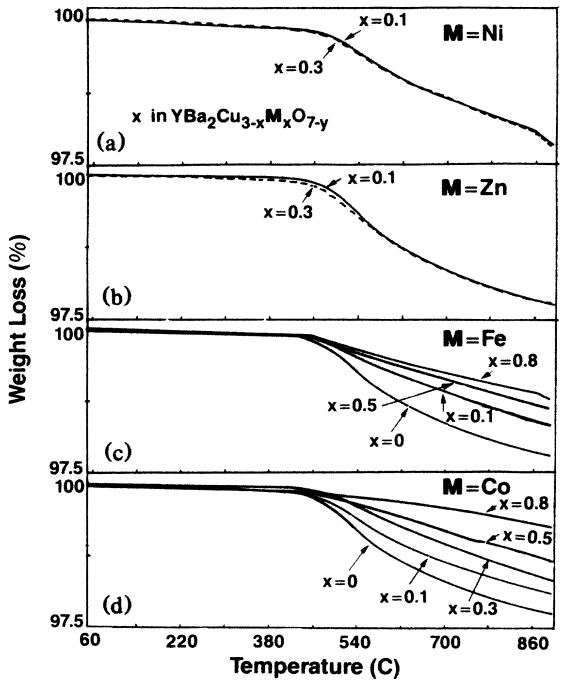

FIG. 5. The oxygen losses are shown as a function of x for the $YBa_2Cu_{3-x}M_xO_{7-y}$ series when the samples are heated under argon up to 900 °C at a rate of 10 °C/min. (a), (b), (c), and (d) refer to the Ni, Zn, Fe, and Co samples, respectively.

C. Neutron powder diffraction

TGA measurements are an indirect way to determine the doping occupancy of Cu(1) and Cu(2) sites. In order to quantify the structure of these substituted high T_c compounds we have performed neutron powder diffraction on two Co-doped samples; $x=0.2$ and $x=0.8$. Neutron data, like x-ray diffraction on the same set of samples, show no evidence for impurity phases. All reflections can be indexed in the tetragonal $P4/mmm$ space group. The powder diffraction data were analyzed by the Rietveld technique which allows the refinement of structural parameters. The known structure of tetragonal $YBa_2Cu_3O_{7-y}$ was used as a starting point in the refinement. All atomic displacements within the cell were allowed to vary, consistent with $P4/mmm$. To include the effects of Co doping, the occupancies of the Co and Cu were allowed to vary, independently, on both Cu(1) and Cu(2) sites, subject to the contraint of complete occupancy of these sites. Since we anticipate changes in oxygen stoichiometry from TGA results, the occupancy of the O(1) site [in the Cu(1) plane] was also allowed to vary in the refinement.

The occupancies obtained from the refinement are shown in Table II, where the x values are in excellent agreement with the concentration used in sample preparation, thus accounting for all of the Co. In addition, the Co preferentially occupies the Cu(1) site, enhancing simul-

TABLE II. Occupancy parameters found from neutron powder diffraction on $YBa_2Cu_{3-x}Co_xO_{6.93-y}$. Co(1) sites are located in the Cu(1) sites between the Ba—O planes, while the Co(2) sites are located in the Cu(2) sites between the Y—Ba planes. O(1) sites are in the Cu(1) plane.

Occupancy	$x=0.2$	$x=0.8$
x	0.22(2)	0.82(2)
Co(1)	0.22(1)	0.73(1)
Co(2)	−0.004(16)	0.098(17)
O(1)	1.04(2)	1.30(2)
$-y$	0.11(2)	0.37(2)

taneously the population of O(1) sites. An interesting finding is that for every two Co atoms substituted in the Cu(1) plane, one additional oxygen is brought into the O(1) site as indicated in Table II. The observed increase in oxygen stoichiometry is consistent with the tetragonal structure, since, higher than fourfold Co-O coordination will introduce oxygen in the a axis sites which would be unoccupied in the orthorhombic structure. These results are also in agreement with the TGA data both for the oxygen content (since for $x=0.8$ we reported $7-y=7.34$) and the occupancy of the Cu(1) sites by Co ions. The thermal parameters for the O(1) site are found to be larger than in the Co-free material, thus, suggesting that the Co–O bond may introduce local static disorder. A detailed discussion of the neutron result will be published elsewhere.[22]

D. Mössbauer data

Mössbauer measurements have been used as a powerful tool to determine unambiguously the oxidation state of the substituted Fe ions as well as their environment (i.e., crystallographic site in the structure).[23–28] The room-temperature Mössbauer absorption spectra of samples with various concentrations x of Fe are shown in Fig. 6. The spectra clearly show the presence of electric quadrupole interactions. Satisfactory fits were obtained in terms of two quadrupole doublets Fe(1) and Fe(2) and a minor absorption doublet Fe(3) in the middle of the spectra. The asymmetry in the line intensities, especially of the two major doublets, may be due to the possible nonrandom orientation of small single-crystal platelets in the powder sample. The fits obtained with three quadrupole doublets were slightly better at higher concentrations of iron. The Fe(3) doublet is much smaller in magnitude and intensity than the other two. The spectra were analyzed by least-squares fitting to a sum of six Lorentzian curves of independent positions, widths, and amplitudes. The parameters obtained from the fits, the quadrupole splitting (QS), and isomer shift (IS) are shown in Table III. If we assume that the substitution of Fe and Cu ions occurs randomly between the Cu(1) and Cu(2) sites, the spectral area of the doublets may be proportional to the relative site occupancies. Therefore we may be tempted to associate Fe(1) and the Fe(2) doublets with the Cu(1) and the Cu(2) sites, respectively, in agreement with Zhou *et al.*[24] This assignment of site preference is not unique; for example Fe may substitute only in Cu(1) site but with different oxygen coordination ranging from 2 to 6, leading to different quadrupolar splittings. The latest assignments are most probable. The intensity ratio of doublet Fe(2) to doublet Fe(1) depends on the iron centration (see Fig. 6). When the concentration of Fe is low, the Fe(1) prevails over the Fe(2). As the Fe concentration increases, Fe(2) prevails over Fe(1). The concentration of Fe(3) is almost constant with x. The isomer shift of the Fe(1) and Fe(2) doublets are very small and close to zero. The isomer shift for the Fe(3) doublet is 0.3 mm/s and is almost independent of the Fe concentration. The IS values indicate that Fe(3) is in Fe^{3+} state. The isomer shifts for the Fe(1) and Fe (2) doublets (Table IV) indicate that Fe could either be localized Fe^{3+} or could be metallic. Mössbauer experiments on sample containing ^{57}Fe as a function of temperature are in progress. We hope to clarify the site assignments and the electronic configuration of Fe in these high T_c superconductor perovskites.

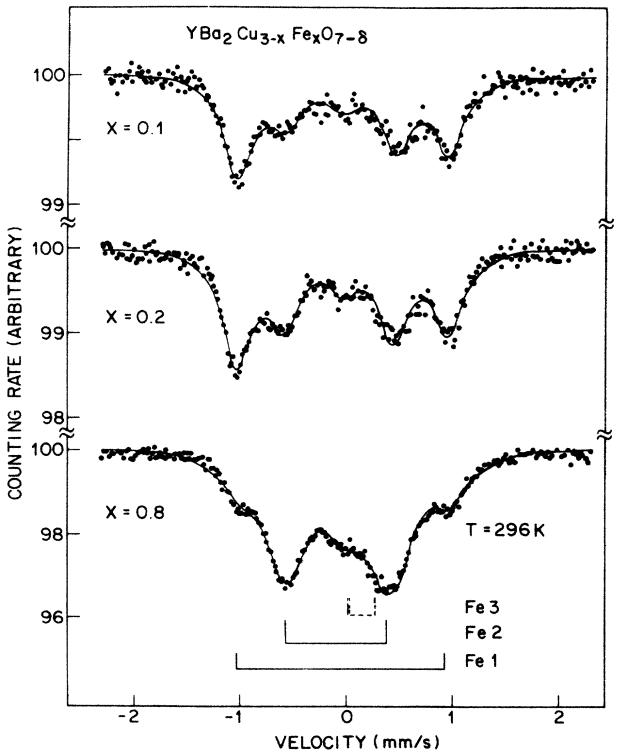

FIG. 6. The Mössbauer spectra collected at room temperature are shown for several members of the $YBa_2Cu_{3-x}Fe_xO_{7-y}$ series ($x=0.1$, 0.2, and 0.8, respectively).

TABLE III. Room-temperature hyperfine parameters (in mm/s) of $YBa_2Cu_{3-x}M_xO_{7-y}$ compounds.

x (Fe)	QS(1)	QS(2)	QS(3)	IS(1)[a]	IS(2)[a]	IS(3)[a]
0.1	1.94	1.10	0.54	0.02	−0.02	0.30
0.2	1.97	1.03	0.56	0.03	−0.02	0.30
0.3	1.98	0.98	0.56	0.05	−0.01	0.31

[a]Isomer shift with respect to Fe metal at room temperature.

E. Superconducting measurements

In Table IV the superconducting critical temperatures determined inductively, T_c(ac), are reported together with those measured resistively where $T_c(\rho)$ and δT_{c0} refer to the resistive midpoint and the transition width, respectively. The width is determined from the 10% to 90% points of the resistive transition. Note that for both the Zn and Ni series, the lowest T_c is 45 K because of the inability to prepare single phase materials for x greater than 0.3. For both the Fe and Co systems, which form a single phase over a wide range of concentration, T_c can be reduced to zero. The resistivity of the Co-doped samples, from room

TABLE IV. Transitions temperatures and resistivity values at 300 K for the materials studied. Also reported are the parameters obtained from a fit to a Curie-Weiss law. Shown are the Weiss constant Θ, the temperature independent susceptibility χ_0, the effective magnetic moment per M atom (μ_{eff}) derived from the Curie constant C, the temperature interval over which the fit was determined, and the rms deviation of the data from the Curie-Weiss law (in percent).

M	x	ρ (300 K) mΩ cm	$T_c(\rho)$ (K)	$\Delta T_c(\rho)$ (K)	T_c (ac) (K)	C_g (emu/g)	σ (%)	Θ (K)	χ_0 (10^{-6} emu/g)	μ_{eff}	μ_{eff} (corrected)	Fitting interval
No	0.00	1.8	91.6	1	93-91	0.5	0.50	21	0.88	...	...	100-300
Fe	0.02	1.7	91.8	1.5	90-88	...	...	...	...	...	...	...
	0.05	1.7	91.8	1.3	90-86	...	...	...	...	...	...	...
	0.1	5.2	76	5	70-55	4.2	0.30	13	0.62	4.74	4.23	T_c-320
	0.2	7.5	49	9	50-34	6.21	0.29	5	1.20	4.05	3.77	T_c-320
	0.3	8	31	7	27-10	8.0	0.20	9	1.49	3.74	3.54	40-320
	0.4	10	<4.2	...	0	10.0	0.29	11	1.83	3.65	3.48	40-320
	0.5	10	0	...	0	12.6	0.27	16	1.87	3.67	3.53	40-320
	0.8	170	0	...	0	14.2	0.14	12	2.90	3.36	3.23	40-320
Co	0.02	1.1	93.4	0.9	92-90	...	...	...	...	...	...	...
	0.05	3.8	94.3	1.4	92-86	...	...	...	...	...	...	...
	0.1	4.5	73	3.7	70-52	3.1	0.16	0	0.71	4.05	3.44	T_c-320
	0.2	11	53	6.2	50-38	5.3	0.18	15	1.14	3.74	3.43	T_c-320
	0.3	20	22	9	13-4	6.4	0.24	20	1.31	3.37	3.14	40-320
	0.4	77	0	...	0	9.7	0.37	52	1.16	3.52	3.28	40-300
	0.5	50	0	...	0	11.2	0.26	66	1.32	3.46	3.31	40-320
	0.8	10^4	0	...	0	16.9	0.58	100	1.23	3.52	3.27	40-320

temperature to 4.2 K, is shown in Fig. 7(a) as an example. Note that T_c decreases continuously with increasing the Co content and is less than 4.2 K at $x=0.4$. Further Co doping results in an increase in resistance with decreasing temperature characteristic of a semiconducting behavior. Note that the tetragonal Co-doped phases where $x=0.1$ and $x=0.2$ show sharp superconducting transition at 75 and 50 K, respectively. Similar results were obtained for the Fe series as summarized in Table IV and shown in Fig. 7(b). For both systems the value of the resistivity above T_c increases with doping content, but more surprising is the incipient semiconducting behavior observed for $x=0.3$. This indicates passage directly from a superconducting to a semiconducting behavior without going through a nonsuperconducting metallic state. Similar results have been so far found in all doping studies of these new high-T_c materials[29] as well as for the Ba-Pb-Bi-O superconducting system.[30] The increase in resistance with decreasing temperature observed just above T_c for the Fe- and Co-doped compounds $x=0.3$ and 0.4, respectively, may be due to inhomogeneities in the sample. However, single-crystal transport measurements[31] show semiconductinglike behavior in the c direction and metalliclike behavior in the (a,b) plane. Therefore, it is also possible that the observed increasing departure from metalliclike behavior in our ceramic samples may reflect localization within the Cu—O planes due to increasing dopant concentration leading to a behavior analog to that observed along the c direction in single crystals. A more detailed study of these effects is in progress.

The variation of T_c as a function of x for the Fe-, Co-, Al-, Ni-, and Zn-doped samples is shown in Fig. 8. Note

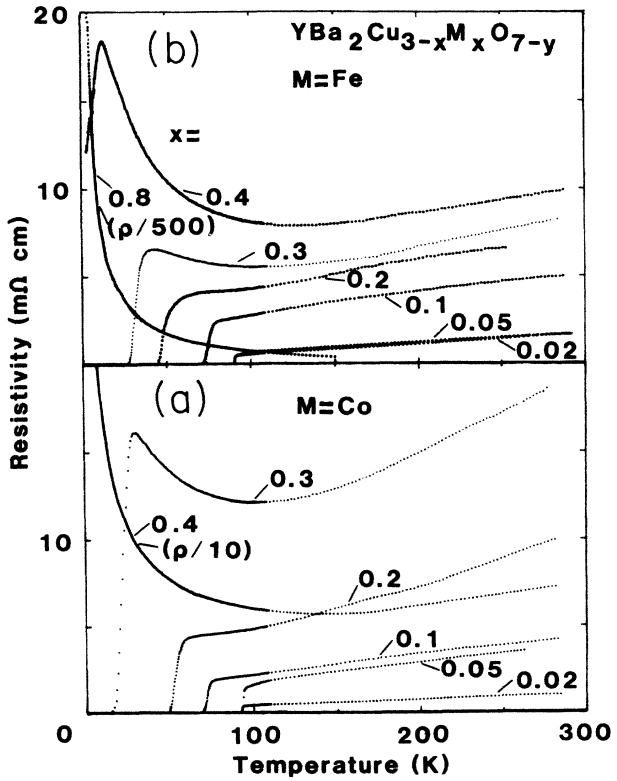

FIG. 7. The resistivity vs temperature for several members of the doped $YBa_2Cu_{3-x}M_xO_{7-y}$ perovskites is given from 300 K to 4.2 K. (a) The data for the Co-doped samples are shown. (b) The data for the Fe-doped samples are shown.

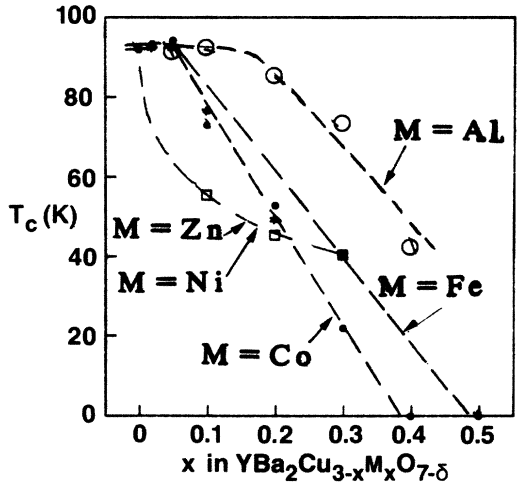

FIG. 8. Variation of the superconducting critical temperatures T_c as a function of x is reported for Fe-, Co-, Ni-, Zn-, and Al-doped 90 K perovskite series.

that the superconducting critical temperatures change in a similar manner for both Fe- and Co-doped samples. T_c remains constant up to $x=0.05$ and then decreases monotonically. The depression of T_c with increasing Ni and Zn concentration is nearly identical. T_c decreases sharply to 55 K at $x=0.1$ and then more slowly to 45 K at $x=0.3$. For greater metal content the system is multiphase. For the Al series, T_c remains constant up to $x=0.1$ where the O-T transition takes place and then decreases continuously up to $x=0.40$. Beyond this Al content the system is multiphase. Independent work[21] on single crystals has shown that T_c was lower than 4.2 K at $x=0.21$. Such a difference may arise from different annealing temperatures or most likely from difficulties in controlling oxygen stoichiometry in single crystals. For instance our $x=0.2$ Al-doped ceramic does not superconduct down to 4.2 K when deficient in oxygen.

The substitution of copper by Fe as reported by Maeno *et al.*[19] shows that the percent of bulk superconductor in their samples decreases with increasing dopant concentration probably due to inhomogeneity effects. Meissner measurements have been done for the Co series and the curves reported in Fig. 9 indicate a similar Meissner effect (of about 38%) is observed for concentrations up to $x=0.2$. This is further evidence that our samples, at least to $x=0.2$, are homogeneous bulk superconductors. For the $x=0.3$ sample, the superconducting transition is not complete, preventing the determination of the exact Meissner fraction. But since the observed effect is smaller than for the other samples of the same series, the material might be less homogeneous, consisting of semiconducting and superconducting grains.

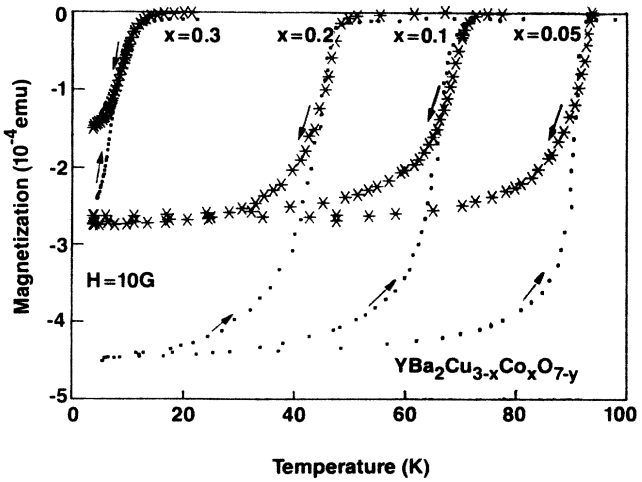

FIG. 9. Magnetic susceptibility as a function of the temperature for several members of the $YBa_2Cu_{3-x}Co_xO_{7-y}$ series. The upper curves are for cooling in a field of 10 G; the lower curves are for warming in 10 G after cooling in zero field.

F. Magnetic measurements

In an attempt to determine the oxidation state of the doped species of the 90-K materials, magnetic measurements have been performed from 4.2 K to room temperature. We present data here only for the Fe and Co system since we have shown elsewhere[18] that Ni, like Zn, is most likely divalent. The observed magnetic susceptibility for two members of each Co and Fe series ($x=0.2$ and $x=0.5$), shown in Fig. 10, indicates that χ_g changes with temperature in a Curie-type manner. The data can be fitted to a Curie-Weiss law of general formula $\chi_g=C_g/(T+\Theta)+\chi_0$, where C_g, Θ, and χ_0 are the Curie constant, the Weiss constant, and the temperature-independent susceptibility. The best fits were usually obtained over the range of temperature 40–320 K. The values of the magnetic moments per doping ions (μ_{eff}) and the Weiss constants deduced from the fits are reported in Table IV, all together with the corrected values of magnetic moments obtained after subtracting out the magnetic contribution for the undoped material. The plot of $(\chi-\chi_0)^{-1}$ vs T (Fig. 10) produces a straight line as expected for a Curie-type behavior. Below 40 K some samples showed a deviation from the Curie law as shown in Fig. 10 for the $x=0.5$ Fe-doped sample, but no evidence for magnetic ordering was observed down to 4.2 K. These anomalies at low temperatures may arise from a small amount of antiferromagnetic impurity phase such as Y_2BaCuO_5 ($T_N=20$ K).[32] However, some type of magnetic ordering was detected by means of low-temperature Mössbauer measurements,[24,28] but the low-temperature behavior might simply reflect an intrinsic property of these compounds, like strong crystal-field interactions.[26] Note that for the Fe series, μ_{eff} per doping atom slightly decreases with increasing the doping concentration whereas it remains roughly independent of the concentration for the Co system. However, a striking result is that the magnetic moment is similar for both Fe and Co ions whereas different values are expected, at least if these ions have the same oxidation state. From this result, it is tempting to state that the magnetic moment is induced on the copper atoms. This point was completely ruled out by

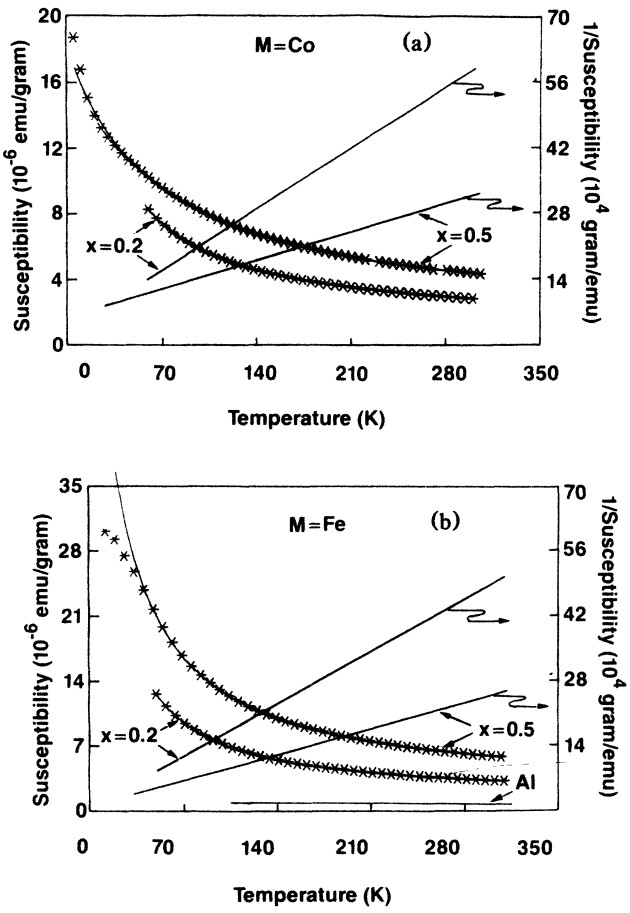

FIG. 10. The magnetic susceptibility in a field of 10 kG as a function of temperature is given for several members of the $YBa_2Cu_{3-x}M_xO_{7-y}$ series [$x=0.2$ and 0.5 when $M=$Co and Fe, (a) and (b) respectively]. In (b) the susceptibility for the Al-doped sample $x=0.2$ is shown as well (dashed curve).

measuring the magnetic susceptibility of the $x=0.2$ Al-doped samples since only a paramagnetic susceptibility independant of the temperature was observed [Fig. 10(b)]. For the Co system, Θ increases with increasing x to reach a value as high as 100 K at $x=0.8$. Crystal-field interactions or impurity phases can be responsible for this negative intercept in the susceptibility $1/\chi$ vs T curve, but the variation of Θ with increasing doping concentration, and the fact that no impurity phase was observed suggests more probably an antiferromagnetic effect. Because of the magnitude of Θ at large x, our simple Curie-Weiss fit may not be very reliable (too much importance should not be attached to μ_{eff}/Co atom at $x=0.8$). High-temperature measurements are required to precisely determine this value. Among the possibilities to explain the antiferromagnetic interactions are dipole-dipole interactions and mediated interactions, for example, via conduction electrons [Ruderman-Kittel-Kasuya-Yosida (RKKY) mechanism] or via cation-anion-cation interactions (superexchange mechanism). The dipole-dipole interactions can be ruled out just because $\Theta=100$ K is unreasonably high for such a kind of interaction. In the RKKY mechanism we should expect Θ to scale with the density of free carriers, but the resistivity experiments [loss of metallicity with increasing doping (see Table III and Fig. 7)] do not give a clear evidence for such a behavior. On the other hand, it is interesting to recall that the sign of the transfer integral for 180° $Co^{3+}-O-Co^{3+}$ superexchange is negative[33] indicating antiferromagnetic interactions. Increasing the Co concentration, results in enhancing the integral transfer and then Θ, as observed. Similar results should be expected with the Fe-doped samples but are not observed, most likely because the Fe is dispersed among both Cu(1) and Cu(2) sites (as indicated above by TGA and Mössbauer data) so that the transfer integral resulting from the 180° superexchange is weakly enhanced. Magnetic measurements have been performed on samples after removal of oxygen and no change in the μ_{eff} was observed, as expected, if the coordinance around Co is not affected by the oxygen removal. The observed deviations from the Curie-Weiss law still persist at low temperatures for the nonsuperconducting argon-annealed samples, suggesting that the "magnetic anomaly" at low temperature is not related to superconductivity. We note here that μ_{eff} was also independent of oxygen content for the rare-earth series.[10] From the μ_{eff}'s alone it is impossible to determine the valence of the doping ions.

DISCUSSION

The $YBa_2Cu_3O_{7-y}$ perovskite structure contains two copper sites. The copper atoms belonging to the Cu–O chains, Cu(1), possess a square-planar environment whereas the ones within the CuO_2 planes, Cu(2), sit in a square-pyramidal environment. The $3d$ metals can occupy either of these sites, and the challenge from the data reported above and related work is to determine the position of the $3d$ metals within the structure and then their oxidation states.

The substitution for Cu by divalent Ni and Zn ions maintains the orthorhombicity of the 90 K phase whereas doping with Fe, Al, and Co ions, which have a higher valence, destroys it and favors a tetragonal unit cell. Chemical pressure is generally required to stabilize $3d$ metals in their high oxidation states (the higher the oxidation state, the smaller the volume of the ion). An ion in a high oxidation state is usually expected to be found in a highly oxygen-coordinated site, for instance, in an octahedral rather than in a square planar environment. The Cu^{3+} ions may constitute an exception if they are on the Cu(1) sites as suggested by other authors, but to our knowledge there are no compounds in which Co^{3+} is square planar. Thus, one would expect cobalt to draw in oxygen atoms in order to increase its coordination. Chemical analysis of oxygen content and neutron measurements as a function of doping content have confirmed this point, at least for x greater than 0.2, and have shown that each added Co atom pulls in 0.5 oxygen atoms, so that a possibility is that two Co atoms may share an oxygen and form Co–O–Co pairs. This would lead to attractive interactions between Co atoms. Such interactions may result in

phase segregation as a function of temperature, thus emphasizing the importance of heating condition. By neutron diffraction it was also shown that Co mainly substitutes for Cu(1) and that extra oxygens occupy the oxygen vacancies present on the a axis in the orthorhombic 90 K phase. The partial filling of these sites induces the tetragonal distortion observed experimentally. A complete occupancy of these sites (octahedral environment) requires one oxygen for each Co atom added [if we assume no oxygen vacancy around Cu(1) is created]. Thus, a cobalt square-pyramidal coordinated (i.e., half of the oxygen vacancies within the a axis occupied) is more suitable to explain the oxygen data. Such a configuration is not unusual for trivalent cobalt and has been found within the $Sr_2Co_2O_5$ phase where the Co atoms sit in an octahedral environment with one oxygen missing (i.e., one oxygen vacnacy[34]). No evidence for a superlattice due to ordering of Co and Cu has been detected by neutron diffraction.

It is important to recall that an O-T transition has been found to occur in these compounds upon removal of oxygen. The structural transition has been explained[35] as the result of the reduction of the effect of repulsive interactions between the oxygens (which force the oxygens to form chains in the 90 K phase starting material) by introducing disorder (i.e., oxygen vacancies). Within the Co-, Al-, or Fe-doped samples the repulsive interactions are overcome by the energy gained to place trivalent ions in an octahedral environment (i.e., 90° O—Co—O bonds). The trivalent ions strongly bond to the oxygen as shown by the TGA measurements which indicate that the number of removable oxygens decreases with increasing dopant content. For instance, only 0.15 oxygen per formula units can be removed from the Co compound with $x=0.8$. The Ni and Zn substitutions do not affect the removal of oxygen; thus we are tempted to claim that divalent Ni and Zn substitute for Cu(2). Neutron diffraction experiments and extended x-ray absorption fine-structure spectroscopy experiments are in progress to answer this question.

At this point an interesting comparison can be made with $YBa_{2-x}La_xCu_3O_{7-y}$ system study by Cava *et al.*[36] The authors have shown that this system undergoes an O-T phase transition at $x=0.4$, and that within the tetragonal range the oxygen content increases with x whereas the amount of removable oxygen decreases with x. Since La cannot substitute for copper, our TGA results may appear at first sight as pure coincidence. It is important to recall that to preserve the charge balance, when La or Co are introduced, either copper must be reduced or oxygen must be added. If we assume the balance of charge to be due only to copper reduction, then the valence of Cu in $YBa_{2-x}La_xCu_3O_7$ will be $(7-x)/3$ and in $YBa_2Cu_{3-x}Co_xO_7$ it will be $(7-3x)/(3-x)$. Then at a given x Cu is more reduced in the La case than in the Co case. But both the O-T transition and the oxygen increase occur at a lower concentration in the Co system than in the La one whereas it should be the contrary if the valence of Cu were responsible for them. Therefore we believe that in the Co system the charge balance is maintained by oxygen uptake resulting from the need of Co to be highly coordinated, rather than by a reduced Cu oxidation state. Thus our TGA results are not fortuitous, and it is the presence of the extra oxygens which drives the structure tetragonal. The sharp change in unit-cell parameters a and c seems to indicate that the O-T transition is discontinuous. On the other hand, because of the insensitivity of diffraction experiments to local order, it may be possible that some of the Cu(1)-O chains may still persist in the tetragonal phase, particularly at the lower Co concentrations where the additional O are localized about the Co impurities. Thus in such a case one would expect a continuous change in the physical properties with increasing doping content, as observed. Our plot of T_c shows a continuous change but with two different slopes which may reflect the rate at which the chains are destroyed within the phase by addition of a trivalent ion.

Explaining the magnetic data for the $3d$ metals is not trivial, mainly because of the various electronic configurations resulting from the competitions between crystal-field and atomic-exchange interactions. For instance, Co^{3+} (d^6) can exist in three electronic configurations which are high spin ($s=2$), low spin ($s=0$), or intermediate spin ($s=1$). With Fe, in addition to different spin states we also have several possible oxidation states (2,3,4,5). Further complications arise from the fact that these compounds are metallic so that the electrons might be slightly delocalized, not residing on the doping atoms M, which would lower the measured effective moment. One intriguing result is that the magnetic moment per doping ion is of about the same order, $\mu_{\text{eff}}=3.4\mu_B$ for both Co- or Fe-doped samples whereas different values will be expected for these d^6 and d^5 ions, respectively. A magnetic moment of $3.4\mu_B$ per either Fe^{3+} or Co^{3+} is, however, too small or too large for high-spin or low-spin configuration, respectively. A similar magnetic moment per Co ion has been obtained for Co^{3+} in an intermediate electronic spin configuration within the perovskite $Sr_2Co_2O_5$ phase where the octahedral environment is distorted due to the presence of an oxygen vacancy.[34] Such an electronic configuration is generally metastable and transforms to high spin at high temperature. To test this hypothesis, magnetic measurements should be extended to higher temperatures but complications may arise from the fact that these compounds lose oxygen when heated above 400 °C. For the cobalt-doped samples it is difficult from magnetic data to ascribe a valence to the Fe ions since the magnetic moment does not correspond to either of the ones expected for the various possible oxidation or electronic states of the Fe ions. But, from the Mössbauer measurements (isomer shift), it seems that Fe is most probably in the Fe^{3+} state as also predicted from structural data. The magnetic moment per Fe atom does not agree either with high-spin ($\sim 5.9\mu_B$) or low-spin ($\sim 2\mu_B$) states. However, the data are consistent with the two following possibilities. First, since Fe is distributed over the two copper sites of different crystal fields, we can have a mixture of high-spin and low-spin configurations. Second, as in the case of Co the value of μ_{eff} may be described by the possibility of an intermediate spin, or spin crossover which is often found in Fe(III) and Co(III), especially in a fivefold coordination.[37]

CONCLUSIONS

We have reported physical properties resulting from the chemical substitution of Cu by Co, Fe, Al, Ni, and Zn in the $YBa_2Cu_{3-x}M_xO_{7-y}$. We show, as for the 40-K materials, that there is a depression of T_c with increasing doping concentration, whether the doping ion is magnetic (Co, Fe, or Ni) or diamagnetic (Al or Zn). This suggests that the behavior of these materials with respect to magnetic impurities is different than that of conventional Bardeen-Cooper-Schrieffer (BCS)-type superconductors. This might be related to the uncommon anisotropic oxide structure of these compounds or to the fact that they may not be conventional BCS-type superconductors. For trivalent ions, an O-T structural transition takes place and, simultaneously, the oxygen content (y) increases whereas for divalent doping (Ni, Zn) both orthorhombicity and oxygen content are maintained. We gave evidence that Co, Fe, and Al substitute mainly in the Cu(1) site, but our data cannot be conclusive for the Ni and Zn substitution. Finally, we stress that the physical properties of these materials are extremely dependent upon processing (i.e., heat treatment time, temperature, and ambient). The unusually short superconducting coherence length (~ 10 Å) of these materials make chemical doping studies quite difficult because of inhomogeneity problems. Work addressing this problem is in progress.

ACKNOWLEDGMENTS

We wish to thank B. G. Bagley, T. Bowmer, T. H. Geballe, M. Giroud, W. R. McKinnon, J. M. Rowell, E. M. Vogel, and J. H. Wernick for helpful discussions and F. J. Rotella and J. D. Jorgensen for their great help in performing the neutron experiments.

[1]M. K. Wu, J. R. Ashburn, C. J. Torng, P. H. Hor, R. L. Meng, L. Gao, Z. J. Huang, Y. Q. Wang, and C. W. Chu, Phys. Rev. Lett. **58**, 908 (1987).

[2]T. P. Orlando, K. A. Delin, S. Foner, E. J. McNiff, J. M. Tarascon, L. H. Greene, W. R. McKinnon, and G. W. Hull, Phys. Rev. B **35**, 7249 (1987).

[3]Y. Le Page, W. R. McKinnon, J. M. Tarascon, L. H. Greene, G. W. Hull, and D. M. Hwang, Phys. Rev. B **35**, 7115 (1987).

[4]J. E. Greedan, A. O'Reilly, and C. V. Stager, Phys. Rev. B **36**, 8770 (1987).

[5]M. A. Beno, L. Soderholm, D. W. Capone, D. G. Hinks, J. D. Jorgensen, J. D. Grace, I. K. Schuller, C. U. Segre, and K. Zhang, Appl. Phys. Lett. **51**, 57 (1987).

[6]J. J. Capponi, C. Chailout, A. W. Hewat, P. Lejay, M. Marezio, N. Nguyon, B. Raveau, J. L. Soubeyroux, J. L. Tholence, and R. Tournier, Europhys. Lett. **3**, 1301 (1987).

[7]W. I. F. David, W. T. A. Harrison, J. M. F. Gunn, O. Moze, A. K. Soper, P. Day, J. D. Jorgensen, M. A. Beno, D. W. Capone, D. G. Hinks, I. K. Schuller, L. Soderholm, C. U. Segre, K. Zhang, and J. D. Grace, Nature **327**, 310 (1987).

[8]F. Beech, S. Miraglia, A. Santoro, and R. S. Roth, Phys. Rev. B **35**, 8778 (1987).

[9]S. Katano, S. Funahashi, T. Hatano, A. Matsushita, K. Nakamura, T. Matsumoto, and K. Ogawa, Jpn. J. Appl. Phys. **26**, L1046 (1987).

[10]J. M. Tarascon, W. R. McKinnon, L. H. Greene, G. W. Hull, and E. M. Vogel, Phys. Rev. B **36**, 226 (1987).

[11]P. K. Gallagher, J. M. O'Bryan, S. A. Sunshine, and D. W. Murphy, Mater. Res. Bull. **22**, 995 (1987).

[12]A. Manthiram, J. S. Swinnea, A. T. Sui, H. Stenifink, and J. B. Goodenough, J. Am. Chem. Soc. **109**, 6667 (1987).

[13]J. D. Jorgensen, M. A. Beno, D. G. Hinks, L. Soderholm, K. J. Volin, R. L. Hitterman, J. D. Grace, I. K. Schuller, C. U. Segre, K. Zhang, and M. S. Kleefisch, Phys. Rev. B **36**, 3608 (1987).

[14]J. M. Tarascon, L. H. Greene, B. G. Bagley, W. R. McKinnon, P. Barboux, and G. W. Hull, in *Novel Superconductivity,* edited by S. A. Stuart and V. Z. Kresin (Plenum, New York and London, 1987), p. 705.

[15]J. M. Tarascon, P. Barboux, B. G. Bagley, L. H. Greene, W. R. McKinnon, and G. W. Hull, in *Chemistry of High Temperature Superconductors*, edited by D. L. Nelson, M. S. Whittingham, and T. F. George (American Chemical Society, Washington, DC, 1987), p. 198.

[16]A. A. Arbrikosov and L. P. Gork'ov, Zh. Eksp. Teor. Fiz. **29**, 1781 (1960) [Sov. Phys. JETP **12**, 1243 (1961)].

[17]L. F. Mattheis and D. R. Hamman, Solid State Commun. **63**, 395 (1987).

[18]J. M. Tarascon, L. H. Greene, P. Barboux, W. R. McKinnon, G. W. Hull, T. P. Orlando, K. A. Delin, S. Foner, and E. J. McNiff, Phys. Rev. B **36**, 8393 (1987).

[19]Y. Maeno, T. Tomita, M. Kyogoku, S. Awaji, Y. A. Oki, K. Hoshino, A. A. Minami, and T. Fujita, Nature **328**, 512 (1987); Y. Maeno, M. Kato, Y. Aoki, and T. Fujita, Jpn. J. Appl. Phys. **26**, L1982 (1987).

[20]G. Demazeau, J. L. Marty, B. Buffat, J. M. Dance, M. Pouchard, P. Dordor, and B. Chevalier, Mater. Res. Bull. **17**, 37 (1982).

[21]T. Siegrist, L. F. Schneemeyer, J. V. Waszczak, N. P. Singh, R. L. Opila, B. Batlogg, L. W. Rupp, and D. W. Murphy, Phys. Rev. B **36**, 8365 (1987).

[22]P. F. Miceli, J. M. Tarascon, L. H. Greene, P. Barboux, F. J. Rotella, and J. D. Jorgensen, Phys. Rev. B **37**, 5932 (1988).

[23]H. Tang, Z. Q. Qiu, Y. W. Du, Gang Xiao, C. L. Chien, and J. C. Walker, Phys. Rev. B **36**, 4018 (1987).

[24]X. Z. Zhou, M. Raudsepp, Q. A. Pankhurst, A. H. Morrish, Y. L. Luo, and I. Maartense, Phys. Rev. B **36**, 7230 (1987).

[25]Z. Q. Qiu, Y. W. Du, H. Tang, J. C. Walker, W. A. Bryden, and K. Moorjani, J. Magn. Magn. Mater. **69**, L221 (1987).

[26]R. Gomez, S. Aburto, M. L. Marquina, M. Jiminez, V. Marquina, C. Quintana, T. Akachi, R. Escuerdo, R. A. Barrio, and D. Rios-Jara, Phys. Rev. B **36**, 7226 (1987).

[27]E. R. Bauminger, M. Kowitt, I. Felner, and I. Nowik, Solid State Commun. **65**, 123 (1988).

[28]T. Tamaki, T. Komai, A. Ito, Y. Maeno, and T. Fujita, Solid State Commun. **65**, 43 (1987).

[29]J. M. Tarascon, L. H. Greene, W. R. McKinnon, G. W. Hull, and T. H. Geballe, Science **235**, 1373 (1987).

[30]B. Batlogg, J. P. Remeika, R. C. Dynes, H. Barz, A. S. Cooper, and J. P. Garno, in *Superconductivity in d- and f-Band Metals*, edited by W. Buckel and W. Weber (Kernforschungszentrum, Karlsruhe, 1982), p. 401.

[31]S. W. Tozer, A. W. Kleinsasser, T. Penney, D. Kaiser, and F. Holtzberg, Phys. Rev. Lett. **59**, 1768 (1987).

[32]S. P. McAlaster *et al.* (unpublished).
[33]J. B. Goodenough, in *Magnetism and the Chemical Bond*, edited by F. A. Cotton (Krieger, Melbourne, FL, 1976), Vol. I, p. 173.
[34]J. C. Grenier, S. Ghodbane, G. Demazeau, M. Pouchard, and P. Hagenmuller, Mater. Res. Bull. **14**, 831 (1979).
[35]W. R. McKinnon, M. L. Post, L. S. Selwyn, G. Pleizier, J. M. Tarascon, P. Barboux, L. H. Greene, and G. W. Hull (unpublished).
[36]R. J. Cava, B. Batlogg, R. M. Fleming, S. A. Sunshine, A. Ramirez, E. A. Rietman, S. M. Zahurak, R. B. van Dover, Phys. Rev. B **37**, 5912 (1988).
[37]F. A. Cotton and G. Wilkinson, *Advanced Inorganic Chemistry* (Wiley, New York, 1980), p. 649.